Advanced Flexible Supercapacitors: Vertical 2D MoS_2 and WS_2 Nanowalls on Graphenated Carbon Nanotube Cotton

Ufuk Perişanoğlu[1*], Esra Kavaz Perişanoğlu[2], Züleyha Kudaş[3], Duygu Ekinci[2], Ismayadi Ismail[4], Emre Gür[5*]

[1]*Faculty of Engineering, Materials Science and Engineering, Hakkari University, Hakkari, Turkey*
[2]*Faculty of Science, Department of Physics, Ataturk University, Erzurum, Turkey*
[3]*Faculty of Science, Department of Chemistry, Ataturk University, Erzurum, Turkey*
[4]*Materials Synthesis and Characterization Laboratory, Institute of Advanced Technology, University Putra Malaysia, Serdang, Malaysia*
[5]*Department of Physics, Faculty of Science, Eskişehir Osmangazi University,26040 Eskişehir, Turkey*

[*] **Corresponding Authors: ufukperisanoglu@hakkari.edu.tr(U. Perişanoğlu)**
emre.gur@ogu.edu.tr (E. Gür)

Electrochemical Measurements;

Specific capacitance, which is one of the most crucial parameters characterizing the electrochemical performance of supercapacitors, can be calculated by utilizing the area under the curve in cyclic voltammetry. This approach provides a quantifiable measure of the supercapacitor's energy storage capacity, reflecting its efficiency and potential for various applications in the field of energy storage technologies.

$$C_{sp,CV} = \frac{1}{mv\Delta V} \int_{0}^{\frac{2\Delta V}{v}} IdV \quad (1)$$

The integral product represents the area between the charge and discharge curves in cyclic voltammetry, where 'm' denotes the mass of the electrode. 'ν' is the scan rate of the cyclic voltammetry program, and 'ΔV' is the voltage window of the experiment. Similarly, this equation can be resolved for specific capacitance by substituting the mass with the area of the active material, resulting in the following equation.

$$C_{A,CV} = \frac{1}{Av\Delta V} \int_{0}^{\frac{2\Delta V}{v}} IdV \quad (2)$$

Similarly, the performance of a supercapacitor electrode can also be calculated using the galvanostatic charge-discharge curves, with the aid of the following equation. This approach enables a precise quantification of the electrode's efficiency in energy storage and release, thereby providing a comprehensive understanding of its operational characteristics in supercapacitor applications.

$$C_{sp,GCD} = \frac{I\Delta t}{m\Delta V} \quad (3)$$

Here, 'I' represents the current, 'Δt' denotes the discharge duration, while 'm' and 'ΔV' are indicative of the mass and voltage windows respectively, as derived from cyclic voltammetry data. This equation, akin to those employed in cyclic voltammetry analyses, can be adapted for utilization where the surface area is considered in lieu of the mass of the material. In this context, 'A' does not refer to the effective surface area of the nanomaterial, but rather, it predominantly pertains to the dimensions of the electrode.

$$C_{A,GCD} = \frac{I\Delta t}{A\Delta V} \quad (4)$$

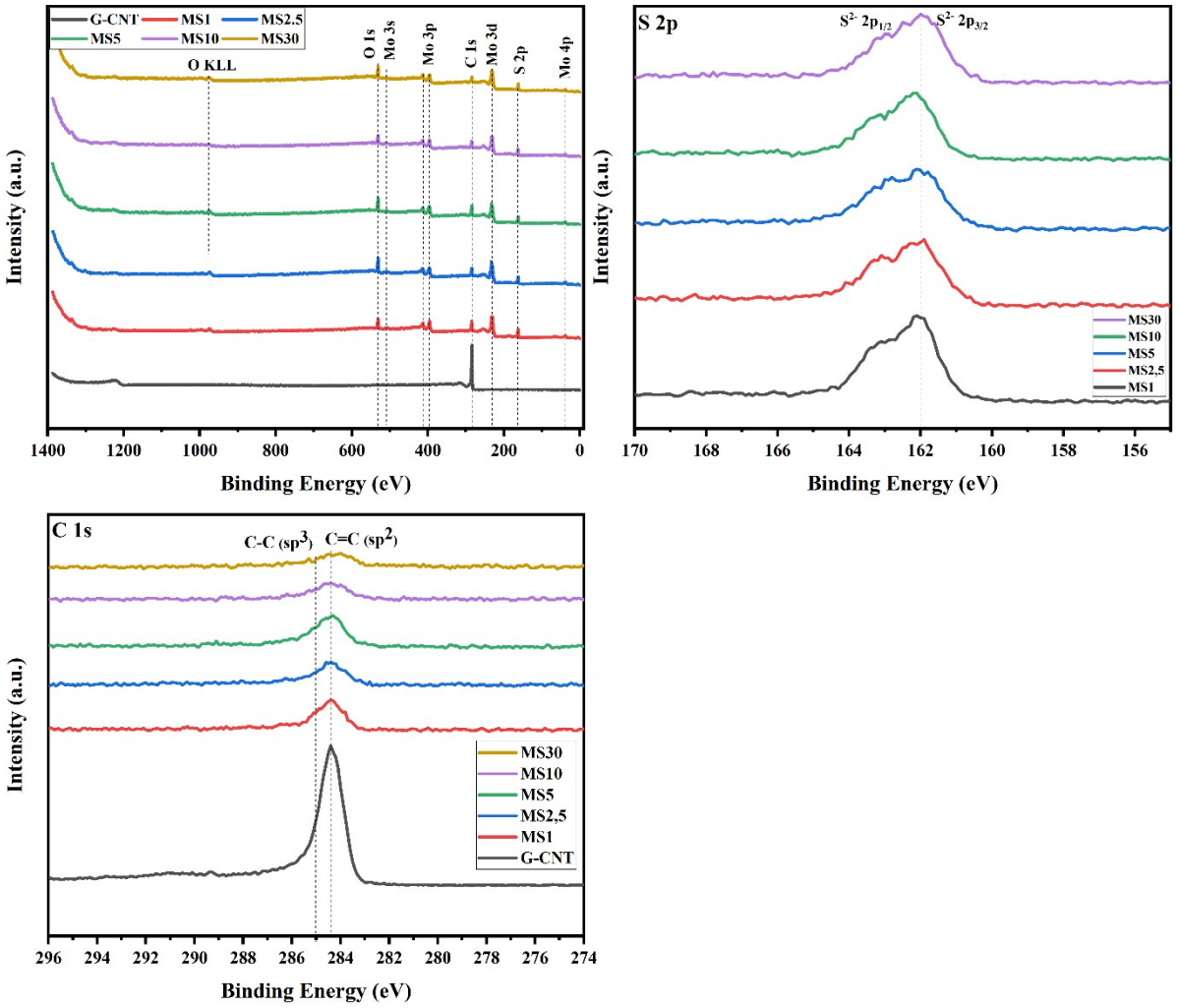

Figure S1. XPS spectra of Mo, S and C measured on the surfaces of MoS_2/G-CNT films with different growth times.

The XPS spectrum belong to G-CNT/MoS_2 structures can be seen above. The survey spectra, high resolution carbon and sulfur core spectra is shown in **Figure S1**. The reflections arising from core level XPS spectra are shown in **Figure S1** for the S 2p special spectrum, exhibiting a spin-orbit splitting of approximately 1.2 eV for S $2p_{1/2}$ and $2p_{3/2}$, resulting in two characteristic doublet peaks for sulfur 2p. In pure G-CNT material, the chemical bonding is observed to consist predominantly of sp^2 hybridized bonds, similar to the structures of graphene and graphite (trigonal planar geometry), as indicated by the peak around 284.4 eV. Additionally, a small amount of sp^3 hybridized bonds is present (peak approximately at 285.5 eV).

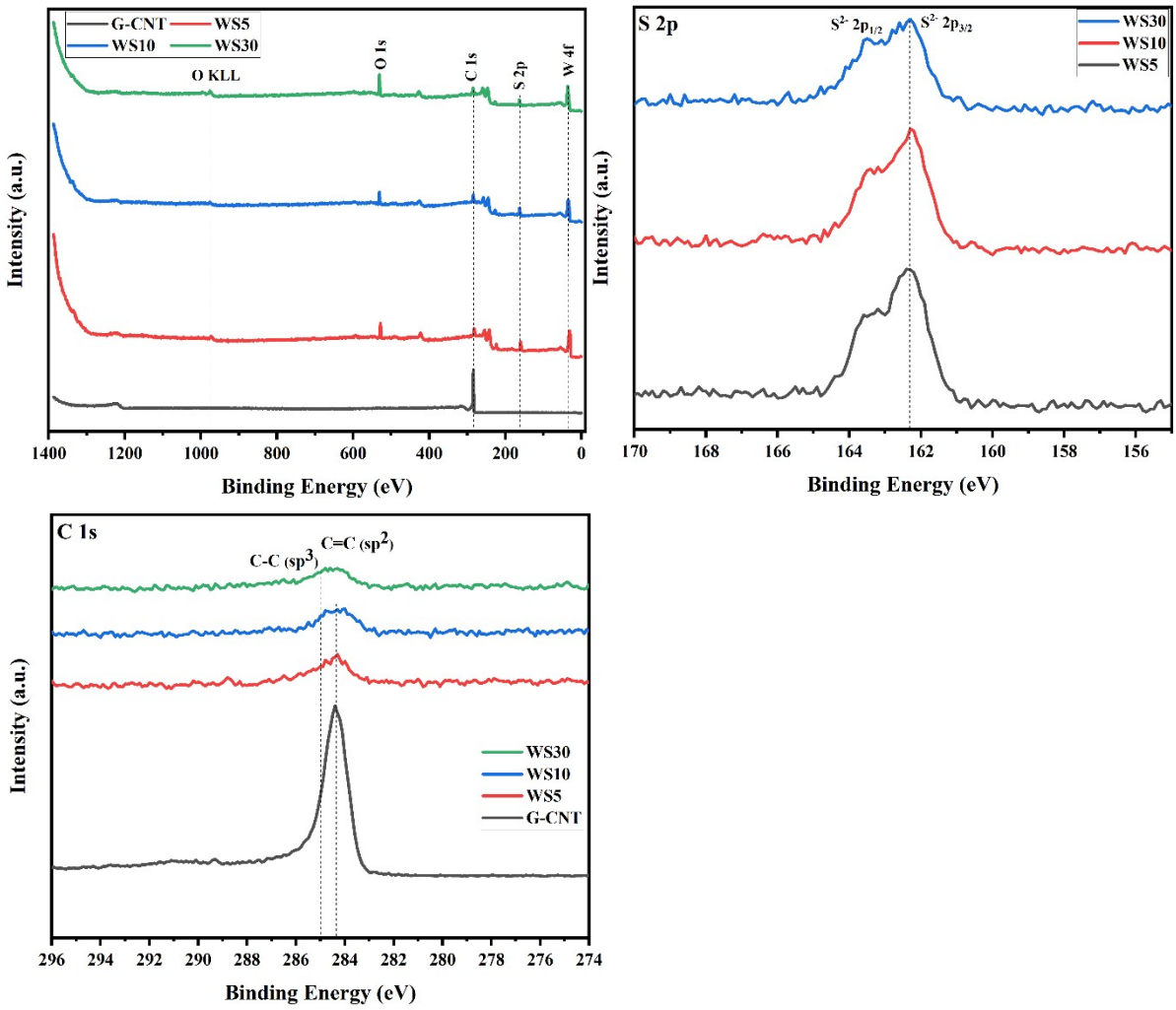

Figure S2. XPS spectra of Mo, S and C measured on the surfaces of WS_2/G-CNT films with different growth times.

The XPS spectrum belong to G-CNT/WS_2 structures can be seen above. The survey spectra, high resolution carbon and sulfur core spectra is shown in **Figure S2**. The peak at 162.3 eV in the S 2p spectrum confirms the presence of S^{2-} in the WS_2/G-CNT hybrid film. Simultaneously, a small amount of oxygen is always present as an impurity in the G-CNT material, suggesting possible reactions with the free bonds of W during the scattering process and growth. The chemical bonding in our pure G-CNT material is found to be composed of dominant sp^2 hybridized bonds (trigonal planar geometry), similar to the structures of graphene and graphite (with a peak at approximately 284.2 eV). Additionally, a small amount of sp^3 hybridized bonds are present (with a peak at approximately 285.1 eV).

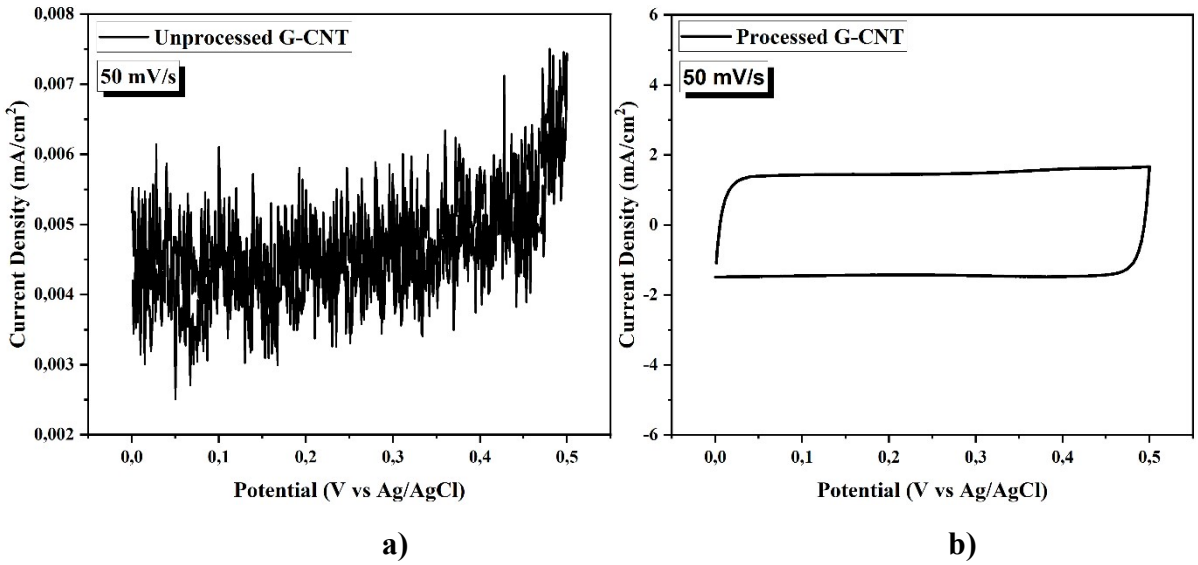

a) **b)**

Figure S3. a) Unprocessed and b) processed G-CNT CV curve

When CV measurements are taken on G-CNT without subjecting it to any treatment, a graph similar to **Figure S3** appears. Due to its hydrophobic structure, immersion in a solution does not yield any CV curve. However, when this material is exposed to oxygen and nitrogen-hydrogen gases at a specific temperature, it becomes hydrophilic, and a cyclic voltammetry curve, as shown in **Figure S3 (b)**, is observed. This indicates that G-CNT transforms into a high-quality electrode and become efficiently wet during solution-based measurements.

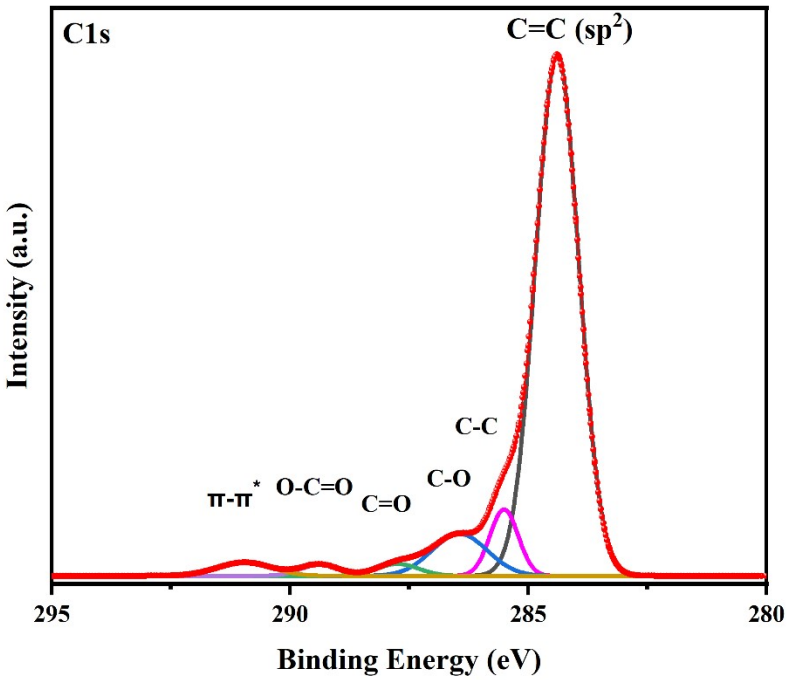

Figure S4. High-resolution XPS spectrum of the C1s region for G-CNT.

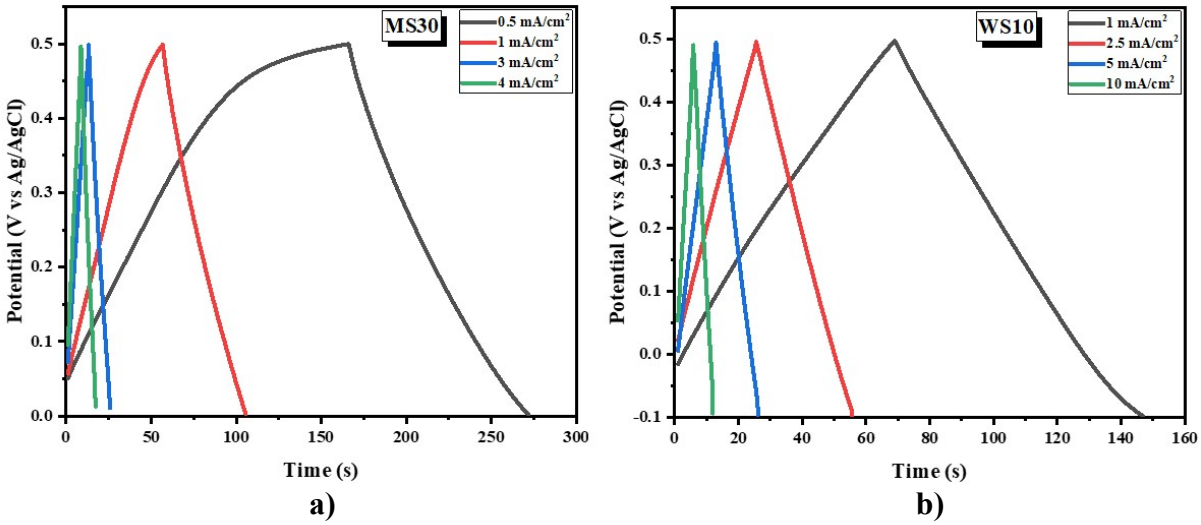

Figure S5. GCD curves of a) MS30 and b) WS10 film at different current densities.

Figure S5 (a) and (b) display the GCD curves for MS30 and WS10 materials grown on G-CNT substrates at various current densities. The capacitance values derived from the GCD curves for both electrodes align well with the specific capacitance values calculated from CV measurements at a scan rate of 50 mV/s.

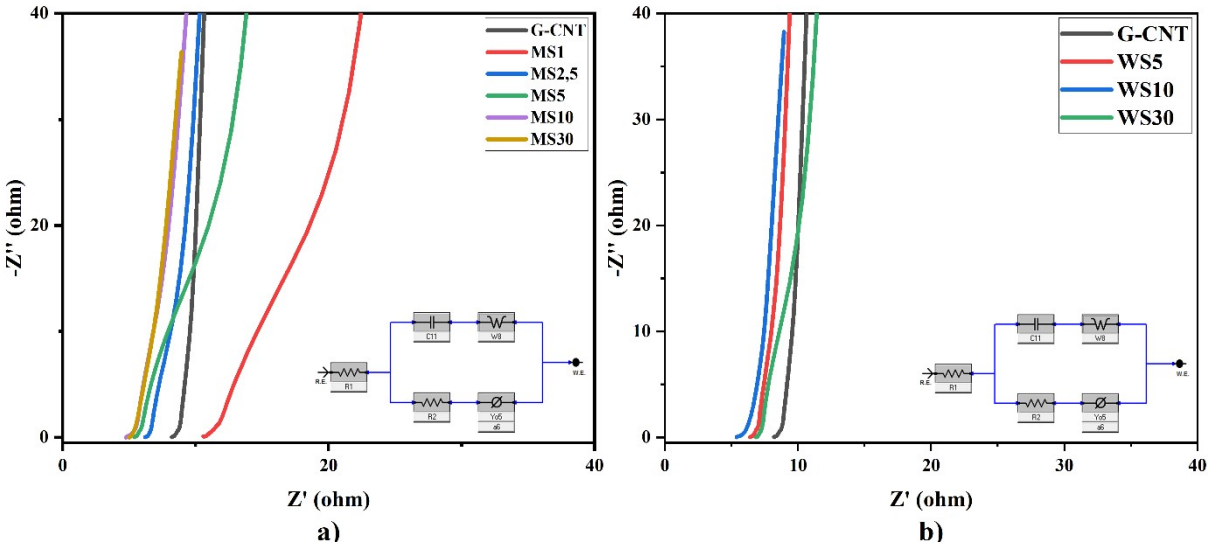

Figure S6. Growth time dependent impedance curves of a) MoS_2/G-CNT b) WS_2/G-CNT films

Considering the performed CV and GCD analyses, it is evident from these two electrodes' high capacitance values, which are also supported by impedance measurements given in **Figure**

S6. The resistance values R_1 and R_2 obtained from EIS analysis of the electrodes are provided in **Table S1**. Equivalent circuit diagrams are included within the figures. Apparently MS30 and WS10 electrodes have shown the lowest resistance values.

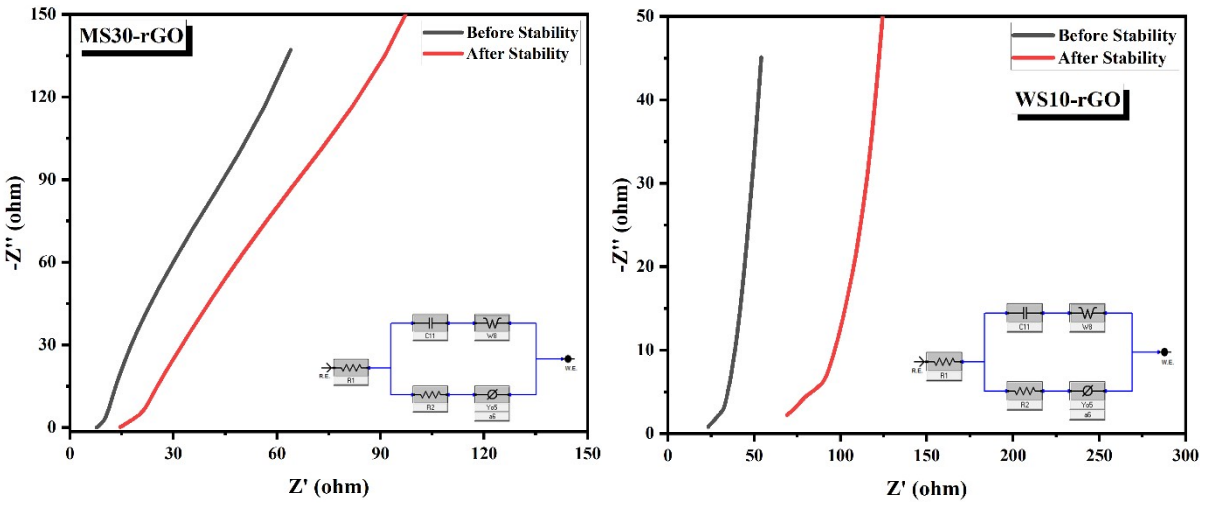

a) **b)**

Figure S7. Impedance measurement before and after stability of **a)** MS30/G-CNT **b)** WS10/G-CNT films

Figure S7 (a) and (b) show the impedance measurements of the MS30 and WS10 devices before and after stability testing, respectively. The obtained resistance values are listed in **Table S2**. As evident from the graph, the resistance values for both devices increased after stability testing. Although there is an change in the R1 and R2 resistance values, the variation is not too significant.

Device application.mp4

Figure S8. Practical application of the WS10-rGO device

Table S1. R1 and R2 Resistance Values of MoS_2 and WS_2 Electrodes.

Electrode	R_1 (ohm)	R_2 (ohm)
G-CNT	8.21	2.19
MS1	10.7	94.0
MS2.5	6.2	0.58
MS5	5.4	89.8
MS10	4.7	1.3
MS30	5.0	0.81
WS5	6.4	2.0
WS10	5.4	2.2
WS30	6.8	0.35

The G-CNT material demonstrated an R1 value of 8.214 Ω, highlighting its high surface conductivity, and an R2 value of 2.185 Ω, indicating low ionic resistance and efficient charge transfer capabilities. These findings confirm the potential of G-CNT as an electrode material, showcasing its excellent electrical conductivity and favorable electrochemical properties, which are critical for supercapacitor applications.

Table S2. Specific Capacitance, Energy and Power Density Values of MS30-rGO and WS10-rGO devices calculated from CV at 50 mV/s scan rate and GCD curves at 1 mA/cm^2 current density.

Device	Specific Capacitance ($C_{S,CV}$, mF/cm^2) 50 mV/s	Capacitance ($C_{S,GCD}$, mF/cm^2) 1 mA/cm^2	Energy Density (μWh/cm^2)	Power Density (mW/cm^2)
MS30-rGO	31.2	53.9	7.49	0.501
WS10-rGO	34.6	80.3	11.1	0.497

Table S3. R_1 and R_2 Resistance Values of MS30-rGO and WS10-rGO Devices.

	Before Stability	After Stability

Device	R_1 (ohm)	R_2 (ohm)	R_1 (ohm)	R_2 (ohm)
MS30-rGO	7.85	358	14.5	6.40
WS10-rGO	23.5	10.6	69.2	23.8